

## Phase transitions in ytterbium under pressure

T G Ramesh, V Shubha and S Ramaseshan

Materials Division, National Aeronautical Laboratory, Bangalore-560017, India

Received 3 September 1976, in final form 13 December 1976

**Abstract.** The semimetal-semiconductor transition in ytterbium has been studied in the pressure range 0–50 kbar and up to 600°C using the Seebeck coefficient as a tool. In the FCC phase, the thermoelectric power exhibits a marked increase with pressure and the semimetal-semiconductor transition is observed as a change in the slope. In the semiconducting phase the thermopower initially increases very rapidly with pressure followed by a steep decrease at higher pressures. The temperature coefficient of thermopower in the semiconducting phase is large and positive in contrast to the semimetallic phase. The FCC-HCP transformation at high temperatures is reported. A semimetal-semiconductor transition in the HCP phase has also been observed. The experimental results are discussed qualitatively on the basis of a simplified two-band model.

### 1. Introduction

The interesting electronic behaviour of ytterbium at high pressures has been investigated by various workers (Souers and Jura 1963, Stager and Drickamer 1963, Jerome and Rieux 1969, McWhan *et al* 1969, Holzapfel and Severin 1971). Souers and Jura (1963) from their resistivity work discovered that ytterbium, which is normally semimetallic becomes a semiconductor above 14 kbar. Much of the subsequent work is concerned with the semimetal-semiconductor transition in the FCC phase of ytterbium. The phase diagram given by Jayaraman (1964) indicates the existence of only the normal FCC phase and a high-temperature BCC phase. However an intermediate HCP phase which is believed to be impurity stabilized (Peterson and Colburn 1966, Spedding *et al* 1966) has been observed and the region of stability of this phase was first reported by Stephens (1965). Recent studies on unstrained and very high purity specimens of ytterbium have revealed the existence of yet another HCP phase below 300 K and 2 kbar (Bucher *et al* 1970, Slavin and Datars 1974). At present it is not established whether these two HCP phases are different or whether the phase boundary in a very pure sample just gets shifted due to impurities.

We report in this paper some new data on the thermoelectric behaviour of Yb in the FCC and HCP phases in the pressure range 0–50 kbar and temperatures up to 600°C. The FCC-HCP phase transformation and the semimetal-semiconductor transition in the FCC and HCP phases have been studied. Using thermopower anomalies as the criterion for phase transitions, we have redetermined the phase diagram of ytterbium. A qualitative explanation of the thermoelectric behaviour is also presented on the basis of a simplified two-band model.

**Table 1.** Mass spectrographic analysis of the impurity elements in Yb.

Impurity	Ca	Eu	Fe	K	Al	Cr	Ti	Ce
Concentration (at %)	0.42	0.19	0.077	0.014	0.014	0.0055	0.0055	0.0053
Impurity	Sm	Y	La	Mn	Zn	Mg	Pb	W
Concentration (at %)	0.0018	0.0016	0.0016	0.0014	0.0013	0.002	0.001	0.001

Pr, Gd, Ta and Cu are present in quantities less than 0.0005%.

## 2. Experimental

Ytterbium samples were cut from an ingot supplied by Research Chemicals, USA and the mass spectrograph analysis of the impurities are as given in table 1. The sample purity is greater than 99.2%.

The x ray diffraction pattern of these samples showed that the material was almost completely in the FCC phase.

High pressures were generated using a piston cylinder apparatus. Pressures up to 50 kbar were obtained in a  $\frac{1}{2}$  in diameter pressure chamber. Thermopower data were collected up to 50 kbar and 200 °C using the Teflon cell technique (Reshamwala and Ramesh 1974) with silicone oil as the pressure transmitting medium. Experiments in the high-temperature region (up to 600°C) were done using a high-temperature-high-pressure thermopower cell (Reshamwala and Ramesh 1975) with talc as the pressure-transmitting medium. All the data presented in this paper of thermopower against temperature or pressure were obtained using an automatic recording system (Shubha and Ramesh 1976).

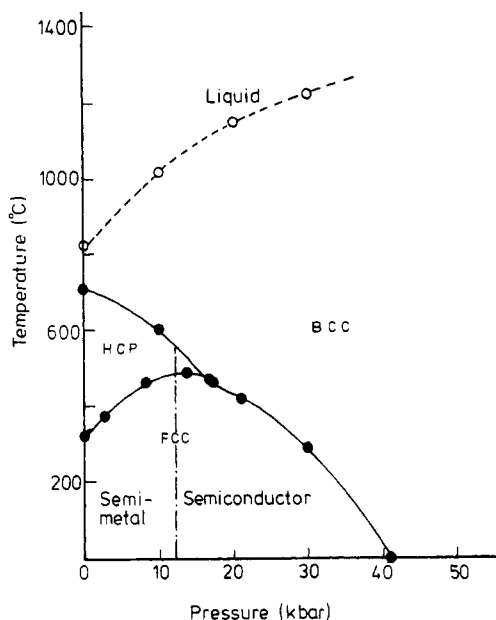
## 3. Results

Figure 1 presents the phase stability diagram of ytterbium, wherein the different solid phase boundaries have been delineated from the present studies of the thermopower anomaly accompanying the transitions. The data on the BCC → liquid phase boundary is due to Jayaraman (1964). In the present investigation we will be mostly concerned with the semimetal-semiconductor transitions in the FCC and HCP phases of Yb. The HCP phase is stable above 300°C and below 15 kbar pressure. The phase diagram constructed out of our thermopower data agrees well with the one determined by Stephens (1965). The semimetal-semiconductor phase boundary in the FCC and HCP phases has also been delineated in figure 1.

### 3.1. Metal-semiconductor transition in FCC Yb

Figures 2 and 3 give the different isotherms of the thermopower against pressure data up to 40 kbar pressure. The main features of the isotherms at 42°C and 94°C (figure 2) are summarized here.

(a) For pressures less than 13 kbar when Yb is semimetallic the thermopower increases rapidly with pressure.



**Figure 1.** Phase diagram of ytterbium, determined using the present thermopower data. (---) approximately demarcates the almost vertical semimetal-semiconductor phase boundary. The bcc-liquid boundary is due to Jayaraman (1964).

(b) The semimetal-semiconductor transition which occurs around 13 kbar pressure is continuous and is observable as a change in the slope of the  $Q$  versus  $P$  graph.

(c) In the semiconducting region (pressure > 13 kbar)  $Q$  initially increases with pressure reaching a maximum and exhibits a rapid decrease after 20 kbar. The rate of decrease of  $Q$  with pressure becomes less rapid at higher temperatures. In the higher temperature isotherm (figure 3) the shoulder characterizing the semimetal-semiconductor transition is absent and, further,  $Q$  increases continuously even up to 40 kbar pressure.

Figure 4 shows some typical isobars of  $Q$  as a function of temperature up to 200 °C. The isobar at 3.7 kbar pressure corresponding to the semimetallic region shows a very small temperature variation of  $Q$ . The higher pressure isobars and especially the one at 31.5 kbar which correspond to the semiconducting region indicate a marked increase of  $Q$  with temperature. The inset in this figure gives the plot of  $Q$  as a function of  $1/T$  at different pressures in the semiconducting phase. It may be noted that the slope of the  $Q$  against  $1/T$  graph is negative and its magnitude increases with increase of pressure. Typical values of the slope are 7.5 mV at 22.3 kbar and 22.5 mV at 35 kbar.

### 3.2. FCC-HCP phase transformation in Yb

Figure 5 gives the high-temperature variation of  $Q$  of Yb at different pressures. The general feature of all these curves is that, above 150 °C,  $Q$  decreases very rapidly with temperature. The temperature coefficient of thermopower at 13.4 kbar is  $-0.128 \mu\text{V}/^\circ\text{C}^2$ . The discontinuous change in  $Q$  at 370 °C and 2.7 kbar pressure corresponds to the first-order phase transition from the FCC  $\rightarrow$  HCP phase. The magnitude

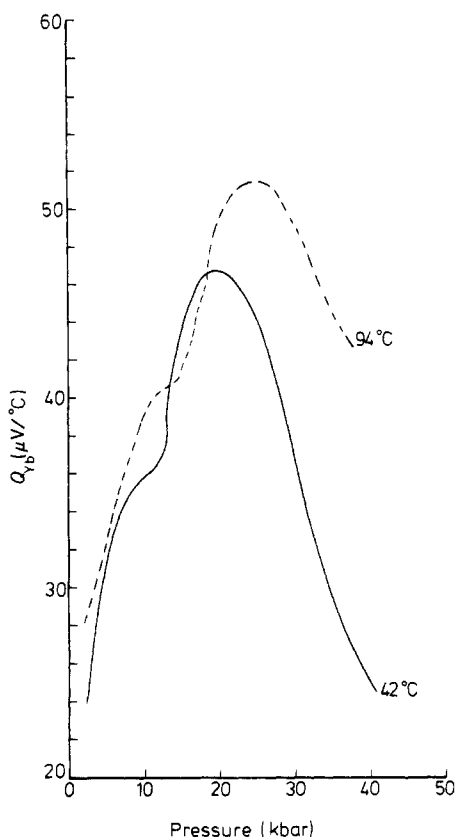


**Figure 2.** Variation of thermopower ( $Q$ ) with pressure in FCC Yb. The shoulders near 13 kbar correspond to the semimetal to semiconductor transition.

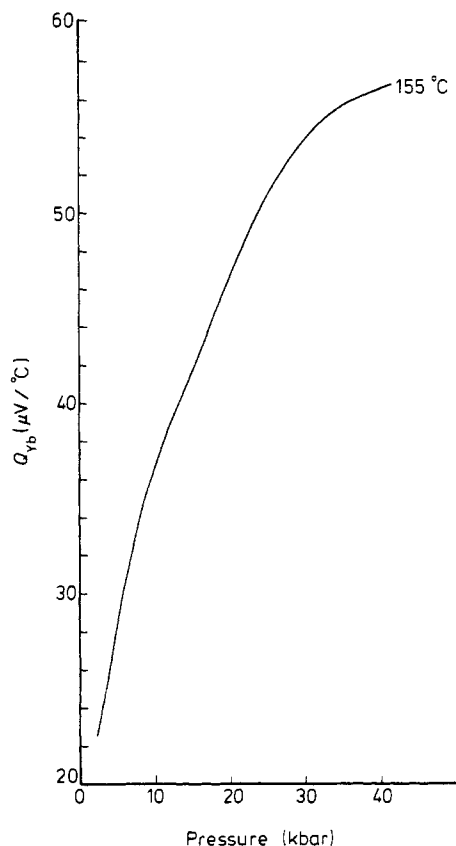


**Figure 3.**  $Q$  against pressure at 155 °C in FCC Yb.

of the anomaly at the phase transition decreases with increase of pressure and the transition temperature increases with increase of pressure. X ray diffraction studies at high temperatures and at atmospheric pressure confirmed the existence of the HCP phase above 300 °C.

### 3.3. FCC–BCC transformation in Yb

Figure 6 gives the isobars of  $Q$  against  $T$  at 17.2 and 21 kbar pressure. Unlike the behaviour shown in figure 5, the magnitude of the anomaly shoots up after 15 kbar pressure and the transformation temperatures decrease with pressure indicating that the phase boundary corresponds to the direct FCC to BCC conversion. This clearly shows that the HCP phase is stable only below 15 kbar pressure.

### 3.4. Semimetal to semiconductor transition in HCP Yb

The pressure behaviour of  $Q$  at different temperatures in the HCP phase of ytterbium are shown in figure 7. To contrast the behaviours in the HCP and FCC phases, isotherms at 300 °C and 400 °C are given in the inset of this diagram. The isotherm

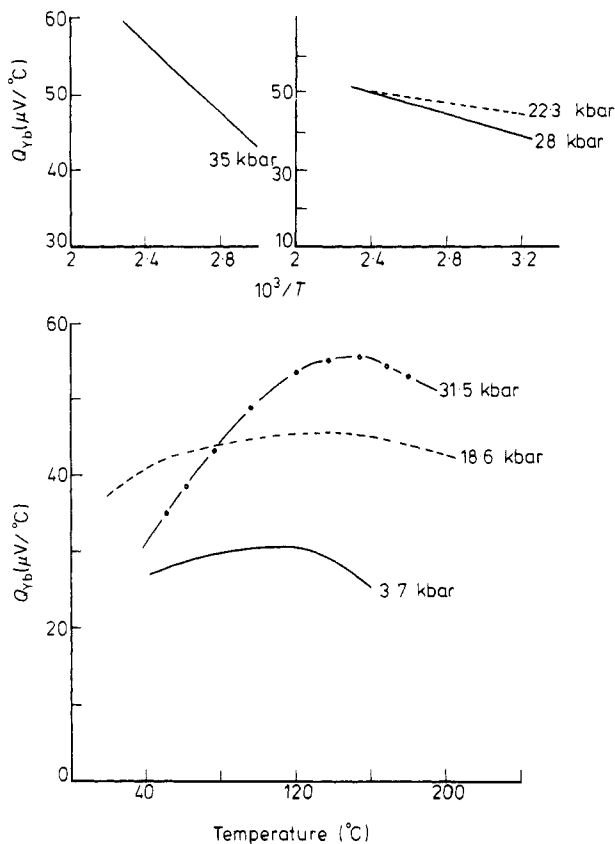


**Figure 4.** Temperature behaviour of  $Q$  in the semimetallic and semiconducting regions of FCC Yb. The inset is a plot of  $Q$  against  $1/T$ . Note the increase in the slope with pressure.

at 300 °C corresponds to the behaviour of Yb when over the entire pressure range it is in the FCC phase. The isotherm at 400 °C shows that for pressures less than 4 kbars  $dQ/dP$  is negative which is characteristic of the HCP phase. The plateau region between 4 kbar and 12 kbar suggests that both FCC and HCP phases, whose thermoelectric behaviour with respect to pressure are opposite, coexist. The coexistence of the two phases is probably due to the inhomogeneous distribution of pressure over the sample encapsulated in a solid pressure-transmitting medium.

The higher temperature isotherms, *viz.* at 450 °C and 475 °C, represent the behaviour when it is in the HCP phase over the pressure region of interest. The semimetal to semiconductor transition occurring around 12 kbar in the HCP phase is more dramatic than that in the FCC phase (see figure 2). Prior to the transition  $Q$  decreases continuously with pressure and  $dQ/dP$  becomes more negative at higher temperatures. The pressure coefficient of thermopower changes sign around 12 kbar which we attribute to a semimetal to semiconductor transition. The large thermopower anomalies observed near 20 kbar at 450 °C and 18 kbar at 475 °C are due to HCP to BCC phase transformation.

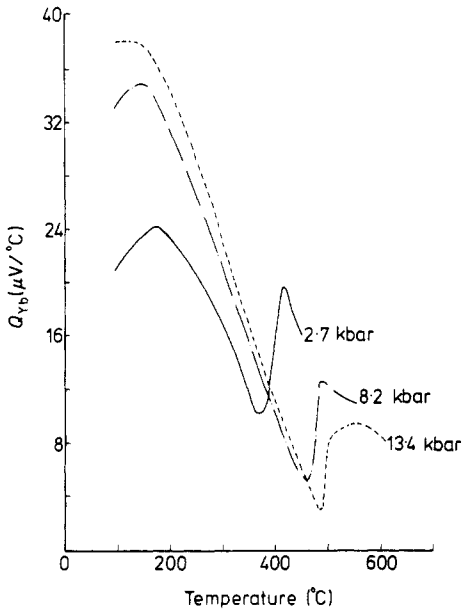


**Figure 5.** FCC-HCP phase transition in ytterbium. The marked decrease of  $Q$  with  $T$  in different isobars may be noted. The discontinuous change in  $Q$  near 375  $^\circ\text{C}$ , 460  $^\circ\text{C}$  and 490  $^\circ\text{C}$  in different isobars corresponds to the FCC-HCP transition.

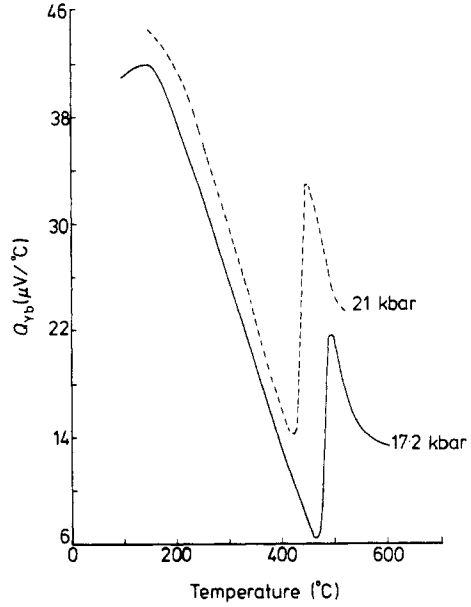


**Figure 6.** FCC-BCC phase transition in ytterbium. The magnitude of the anomaly is large compared to that in the previous figure.

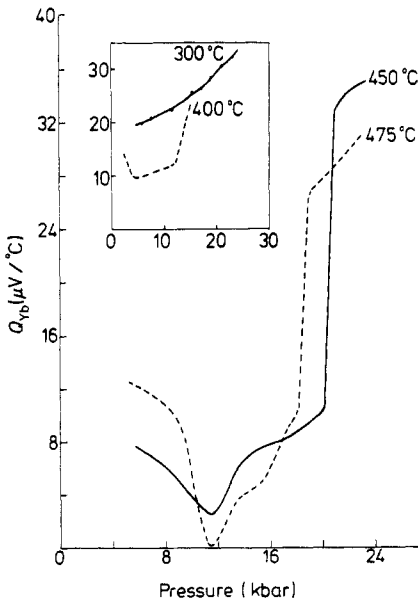


**Figure 7.** Metal-semiconductor transition near 13 kbar in HCP ytterbium. The large and discontinuous change in  $Q$  near 18 and 20 kbar in the two isotherms is due to the HCP-BCC phase transition. The isotherm at 300  $^\circ\text{C}$  given in the inset corresponds to the behaviour in the pure FCC phase. The curve at 400  $^\circ\text{C}$  gives the behaviour when both HCP and FCC phases coexist.

## Discussion and conclusions

The two-band model developed for Yb and similar divalent metals such as Ca and Sr has been discussed by several authors (Mott and Jones 1936, Vasvari *et al* 1967, Johansen and Mackintosh 1970). The basic feature of the energy band model for Yb is that at atmospheric pressure there is a small overlap between the filled 6s band and the empty 5d band. The schematic energy band diagram of ytterbium as a function of pressure can be found in an article by Gschneidner (1964). The transport properties of ytterbium suggest that it is semimetallic at lower pressures (less than 12 kbar). Near 13 kbar this overlap is removed resulting in the semimetal to semiconductor transition (Souers and Jura 1963).

The experimental results on the thermoelectric behaviour of Yb in the FCC and HCP phases can be qualitatively understood on the basis of the above two-band model. The Seebeck coefficient of FCC Yb at atmospheric pressure is large and positive of the order of  $+22\mu\text{V}/^\circ\text{C}$ . This correlates with the measured Hall coefficient  $R_H \approx +7 \times 10^{-9} \text{ m}^3/\text{C}$  (Holzapfel and Severin 1970). The sign of the Hall coefficient has been interpreted in the light of the two-band model as due to the mobility of the holes being greater than that of the electrons (Jerome and Rieux 1969, Holzapfel and Severin 1970). The positive sign of  $Q$  is in conformity with the Hall effect data and the relatively large magnitude of  $Q$  is simply due to the small carrier concentration.

The increase of  $Q$  with pressure in the semimetallic region (figure 2) is mainly due to the gradual removal of the band overlap and the consequent decrease in the carrier concentration. This is in conformity with the continuous increase in the resistivity with pressure (Souers and Jure 1963) and the Hall coefficient variation with pressure in the FCC phase (Holzapfel and Severin 1970).

The semimetal to semiconductor transition in the FCC phase is observable as a shoulder in the  $Q$  against pressure graph (figure 2). The steep initial increase and the subsequent decrease in the magnitude of  $Q$  with pressure which is conspicuous in the  $42^\circ\text{C}$  isotherm suggests that there are two opposing contributions to the diffusion thermopower. The general expression for the diffusion thermopower of a semiconductor in the intrinsic region is given by (Tauc 1962, Johnson and Lark-Horovitz 1953)

$$Q = \frac{-k}{|e|} \left[ \left( \frac{C-1}{C+1} \right) \frac{E_0}{2kT} + \left( \frac{C-1}{C+1} \right) \frac{a}{2k} + \frac{3}{4} \ln \frac{m_n}{m_p} + \frac{C}{C+1} \frac{Q_n^*}{kT} - \frac{1}{C+1} \frac{Q_p^*}{kT} \right] \quad (1)$$

where  $C$  is the mobility ratio of electrons to holes,  $E_0$  = energy gap at 0 K,  $a$  = temperature coefficient of variation of the energy gap,  $m_n$  and  $m_p$  = effective masses of electrons and holes respectively,  $Q_n^*$  and  $Q_p^*$  = heats of carrier transfer.

Assuming that the main scattering mechanism is through lattice vibration, we get  $C^{2/5} = m_n/m_p$ . Thus the main parameters which enter the expression for  $Q$  are  $E_0$ ,  $C$  and  $a$ . Qualitatively the initial increase of  $Q$  with pressure after the transition (figure 2) may be understood by noting that the first term makes a negligible contribution ( $E_0$  being extremely small) while the effective mass term predominates. At higher pressures, the negative contribution to  $Q$  from the first term becomes increasingly

important and accounts for the rapid decrease of  $Q$  with pressure. On the same hypothesis the behaviour of the isotherm at 155 °C (figure 3) can be understood.

It is clear from equation (1) that a complete quantitative analysis of the experimental data is not possible in the absence of other information like the Hall coefficient at high temperatures and high pressures and magnetoresistance. However, we present some order of magnitude calculations on the mobility ratio and the temperature coefficient of variation of the energy gap. In the pressure region of interest, the energy gap is very small (0.05 eV at 35 kbar) and has been estimated to vary at the rate of 30 K kbar<sup>-1</sup> (Jerome and Rieux 1969) after the semimetal to semiconductor transition. Thus in the temperature range 300 K–500 K there will be enough thermally excited carriers in the conduction band and hence the material can be considered to be in the intrinsic regime.

The increase in the magnitude of thermopower with temperature (figure 4) suggests that the carriers are partially degenerate. The Hall coefficient at 300 K becomes negative at 20 kbar pressure and its magnitude increases with pressure after the semimetal to semiconductor transition. (Holzaphel and Severin 1970). This suggests that  $C$  is greater than unity and increases with pressure. The bandstructure calculations also suggest that the effective mass of 5d electrons decreases strongly with pressure while that of 6s holes is not much affected. Since  $m_p \gg m_n$ , the chemical potential will shift towards the conduction band with increase of temperature and hence the electron gas would become degenerate. However the holes in the valence band remain nondegenerate and make a large contribution to the thermopower. The sign of thermoelectric power would thus be positive in spite of the fact that the electron mobility is greater than that for holes.

The slope of the  $Q$  against  $1/T$  plot over a limited temperature range between 350 K–500 K yields the values of  $C$  which are tabulated in table 2. Here we have utilized the energy gap values given by Souers and Jura (1963). It may be noted that  $C$  is positive and increases with pressure. From the intercept and these  $C$  values, the parameter  $a$  which determines the temperature variation of the energy gap have been evaluated and are given in table 2. The value of  $a$  is of the same order of magnitude as that of Ge (Johnson and Lark-Horovitz 1953). Combining the value of  $C$  and  $R_H$  at different pressures, the carrier concentration  $n$  at 300 K can be evaluated using the relation

$$R_H = - \frac{1}{n|e|} \frac{C - 1}{C + 1} \quad (2)$$

The carrier concentration at different pressures are given in table 3.

The large and linear decrease of  $Q$  with temperature in the semimetallic region (figure 5) is due to the thermal excitation of carriers across the overlapping region

**Table 2.** The parameters  $C$  and  $a$  at different pressures extracted from the  $Q$  against  $1/T$  plot.

Pressure (kbar)	$E_{\text{gap}}$ (eV)	Slope of $Q$ against $1/T$ (V)	$C = \mu_e/\mu_h$	$a(\text{eV}/^\circ\text{C})$
22.3	0.025	$-0.75 \times 10^{-2}$	4.16	$-4.09 \times 10^{-4}$
28.0	0.04000	$-1.25 \times 10^{-2}$	4.52	$-4.05 \times 10^{-4}$
35.0	0.07050	$-2.25 \times 10^{-2}$	4.82	$-4.3 \times 10^{-4}$



**Table 3.** Carrier concentrations at different pressures obtained from the  $C$  values and the Hall effect data.

Pressure (kbar)	$R_{11}(\text{cm}^3/\text{C}^{-1})$	Electron (hole) concentration at 300 K	No. of electrons (holes)/atom at 300 K
22.3	$-1 \times 10^{-4}$	$3.82 \times 10^{22}$	1.576
28	$-5 \times 10^{-4}$	$1.28 \times 10^{22}$	0.53
35	$-7.5 \times 10^{-4}$	$0.875 \times 10^{22}$	0.36

of 6s and 5d bands. The decrease suggests that the electron contribution to the diffusion thermopower becomes increasingly important at higher temperatures. The isobars (figure 6) appropriate to the semiconducting phase show a similar behaviour and the same explanation holds good. It may be noted that the linear variation of  $Q$  with temperature implies that the carrier are becoming degenerate in this temperature range.

The pressure variation of thermopower in the HCP phase of Yb (figure 7) is qualitatively different from that in the FCC phase. The continuous decrease of  $Q$  prior to semimetal to semiconductor transition suggests that the mobility of electrons is a strong function of pressure and the very small magnitude of  $Q$  at the transition ( $\sim 0\mu\text{V}/^\circ\text{C}$ ) in the  $475^\circ\text{C}$  isotherm is indicative of the close compensation of the electron and the hole contributions. The most important feature in the HCP phase is that the magnitude of thermopower is extremely small even in the semiconducting phase and it may be appropriate to consider it as a degenerate semiconductor.

We may conclude by summarizing as follows. The semimetal to semiconductor transition in the FCC and HCP phases of Yb has been studied using thermopower as a tool. The FCC  $\rightarrow$  HCP  $\rightarrow$  BCC phase transformations have also been studied. The experimental results have been interpreted on the basis of a two-band model appropriate to ytterbium.

## Acknowledgments

The authors thank Mr K Jagannatha Rao and Mr V Venu for the technical help, Professor V S Venkatasubramaniam, Mr P T Rajagopalan and Mr M Kalyanam for the mass spectrographic analysis of the sample and Dr Kalyani Vijayan and Mr Mani for the x ray work. One of us (VS) gratefully acknowledges CSIR (India) for the grant of a research fellowship.

## References

- Bucher E, Schmidt P H, Jayaraman A, Andres K, Maita J P, Nassan K and Dernier P D 1970 *Phys. Rev.* **B 2** 3911
- Gschneidner K A 1964 *Rare Earth Research* vol III (New York: Gordon and Breach)
- Holzappel W B and Severin D 1971 *Phys. Lett.* **34** A 371
- Jayaraman A 1964 *Phys. Rev.* **135** A 1056
- Jerome D, Rieux M 1969 *Solid St. Commun.* **7** 957
- Johansen G and Mackintosh A R 1970 *Solid St. Commun.* **8** 121
- Johnson V A and Lark-Horovitz K 1953 *Phys. Rev.* **92** 226

- McWhan D B, Rice T M and Schmidt P H 1969 *Phys. Rev.* **177** 1063
- Mott N F and Jones H 1936 *Theory of Properties of Metals and Alloys*. (London: Oxford University Press)
- Peterson D T and Colburn R D 1966 *J. Phys. Chem.* **70** 468
- Reshamwala A S and Ramesh T G 1974 *J. Phys. E: Sci. Instrum.* **7** 133
- 1975 *J. Phys. E: Sci. Instrum.* **8** 465
- Shubha V and Ramesh T G 1976 *J. Phys. E: Sci. Instrum.* **9** 435
- Slavin A J and Datars W R 1974 *Can. J. Phys.* **52** 1622
- Souers P C and Jura G 1963 *Science* **140** 481
- Spedding F H, Hanak J J and Daane A H 1961 *J. Less-Common metals* **3** 110
- Stager R A and Drickamer H G 1963 *Science* **139** 1284
- Stephens D R 1965 *J. Phys. Chem. Solids* **26** 943
- Tauc J 1962 *Photo- and Thermoelectric Effects in Semiconductors* (Oxford: Pergamon Press)
- Vasvari B, Animalu A O E and Heine V 1967 *Phys. Rev.* **154** 535